European Journal of Neuroscience, Vol. 16, pp. 197–208, 2002 *© Federation of European Neuroscience Societies*

Early sequential formation of functional $GABA_A$ and glutamatergic synapses on CA1 interneurons of the rat foetal hippocampus

Sonia Hennou, Ilgam Khalilov, Diabé Diabira, Yehezkel Ben-Ari and Henri Gozlan
INMED-INSERM Unité 29, Université de la Méditerranée, 163, route de Luminy, BP 13, 13273 Marseille cedex 9, France

Keywords: morphofunctional studies, peridendritic interneurons, perisomatic interneurons, sequential synapse formation

Abstract

During postnatal development of CA1 pyramidal neurons, GABAergic synapses are excitatory and established prior to glutamatergic synapses. As interneurons are generated before pyramidal cells, we have tested the hypothesis that the GABAergic interneuronal network is operative before glutamate pyramidal neurons and provides the initial patterns of activity. We patch-clamp recorded interneurons in foetal (69 neurons) and neonatal P0 (162 neurons) hippocampal slices and performed a morphofunctional analysis of biocytin-filled neurons. At P0, three types of interneurons were found: (i) non-innervated 'silent' interneurons (5%) with no spontaneous or evoked synaptic currents; (ii) G interneurons (17%) with $GABA_A$ synapses only; and (iii) GG interneurons with GABA and glutamatergic synapses (78%). Relying on the neuronal capacitance, cell body size and arborization of dendrites and axons, the three types of interneurons correspond to three stages of development with non-innervated neurons and interneurons with $GABA_A$ and glutamatergic synapses being, respectively, the least and the most developed. Recordings from both pyramidal neurons and interneurons in foetuses (E18–20) revealed that the majority of interneurons (65%) had functional synapses whereas nearly 90% of pyramidal neurons were quiescent. Therefore, interneurons follow the same GABA–glutamate sequence of synapse formation but earlier than the principal cells. Interneurons are the source and the target of the first synapses formed in the hippocampus and are thus in a position to modulate the development of the hippocampus in the foetal stage.

Introduction

The formation of the network is associated with two fundamental features of GABAergic synapses, as follows.

(i) GABA is excitatory at early developmental stages, a fundamental property that has been initially observed in the rat hippocampus (Ben-Ari *et al*., 1989) and subsequently in several species and brain regions (reviewed in Ben-Ari, 2001). In keeping with this, activation of GABAergic synapses generates action potentials (Khazipov *et al*., 1997), removes the voltage-dependent magnesium block from NMDA channels (Leinekugel *et al*., 1997), and elevates the concentration of $[Ca^{++}]_i$ (Leinekugel *et al*., 1995; Segal, 1993) in the hippocampus and in other brain structures (see Ben-Ari, 2001). These effects may underlie the well-characterized modulation by GABA of activity-dependent developmental processes including neuronal growth (LoTurco *et al*., 1995), neuronal differentiation (Belhage *et al*., 1998), proliferation and migration (Behar *et al*., 1996; Barker *et al*., 1998), growth rates of neuronal processes (Barbin *et al*., 1993; Belhage *et al*., 1998) and synapse formation and clustering (Davies *et al*., 1998; Khazipov *et al*., 2001).

(ii) GABAergic synapses are formed before glutamatergic synapses on pyramidal neurons of the hippocampus of neonatal rodents (Tyzio *et al*., 1999) and embryonic primates (Khazipov *et al*., 2001). This suggests that at an early developmental stage GABAergic synapses may provide all the information received by immature pyramidal neurons. Therefore, if GABAergic synapses are formed prior to the glutamatergic synapses on the principal cells, then the interneuronal network would be expected to develop earlier than pyramidal neurons. As a consequence, such a network may provide the earliest patterns of activity in the developing hippocampus and play a crucial role of in the generation of patterns and oscillations (Buzsaki, 1997). In keeping with this, there is a dominant pattern of activity in the developing hippocampus, the giant depolarizing potentials (GDPs), which are generated primarily by the excitatory actions of GABAergic synapses (Ben-Ari *et al*., 1989; Ben-Ari, 2001). At present, however, there is not enough data on the maturation of interneurons (see Lang & Frotscher, 1990) and the early establishment of functional synapses to substantiate this hypothesis.

We have therefore addressed this issue and our aims were first to determine whether the GABA–glutamate sequence is also valid for interneurons in order to better understand whether this rule applies to all populations of hippocampal neurons independently of their postsynaptic target. Our second aim was to compare the sequential formation of GABA and glutamatergic synapses in interneurons and pyramidal neurons. Indeed, if interneurons divide and become functional prior to pyramidal neurons, they may have spontaneous synaptic currents at a time when pyramidal neurons are silent and thus exert a central role in the development of the principal cells. In the present study we report that, in CA1 interneurons, GABAergic synapses are formed prior to glutamate ones and that the interneuronal network is already operative *in utero* at a time when

Correspondence: Dr H. Gozlan, as above.
E-mail: gozlan@inmed.University-mrs.fr

Received 13 March 2002, accepted 16 May 2002

doi:10.1046/j.1460-9568.2002.02073.x

pyramidal neurons are primarily quiescent. We also provide for the first time a description of the morphology of a large population of physiologically identified immature interneurons.

Materials and methods

Experiments were performed on CA1 hippocampal slices obtained from Wistar rats. All protocols were designed according to INSERM guidelines for the care and use of animals. Female rats were mated overnight, the day of insemination being at embryonic day (E)0. Birth usually occurred on E22 and was designated as postnatal day (P)0. E18–20 embryos were removed by caesarean section after ether anaesthesia of the mother. P0 animals were killed < 6 h after birth.

Slice preparation

Rats were decapitated and brains were removed and placed in oxygenated ice-cooled artificial CSF (ACSF) with the following composition (in mM): NaCl, 126; KCl, 3.5; $CaCl_2$, 2; $MgCl_2$, 1.3; $NaHCO_3$, 25; $NaHPO_4$, 1.2; glucose, 10. Hippocampal transversal slices (400 μm) were cut using a Vibratome (VT 1000E; Leica, Nussloch, Germany) and kept in oxygenated ACSF (95% O2 and 5% CO2; pH 7.3) at room temperature for at least 1 h before use. Slices corresponding to the middle third were generally taken for patch-clamp experiments. Individual slices were then transferred to the recording chamber where they were fully submerged and super-fused with oxygenated ACSF at 31 ± 1 °C at a flow rate of 3.5 ± 0.1 mL/min.

Electrophysiological recordings

Stimulation of the afferent pathway was achieved with a bipolar twisted nichrome electrode, placed in stratum radiatum (SR) or in stratum oriens (SO) of CA1. To cover most of the surface, the two branches (50 μm diameter each) of the stimulating electrode were separated at the tip so that one of the branches was placed at the border of stratum pyramidale (SP) and the other one close to stratum lacunosum moleculare (SLM) or the alveus. The stimulation was applied to the slice with an intensity of 30–60 V and duration of 30 μs and at a frequency of 0.033 Hz. In the case of non-innervated cells, the stimulating intensity was increased up to 90 V. Interneurons were patched in all CA1 areas including the pyramidal layer, but the highest number of cells was recorded in SR. Patch-clamp experiments were usually performed blindly using the whole-cell configuration (Hamill *et al.*, 1981) with either Axopatch 200B (Axon instruments, Foster City, CA, USA) or EPC9 (HEKA, Germany) amplifiers. In a small number of slices, interneurons were also patched under visual control (Zeiss Axioscope microscope and a Hamamatsu camera with an incident light filtered to pass visible and infrared).

Patch pipettes were filled with a potassium gluconate solution to simultaneously visualize $GABA_A$ and AMPA receptor-mediated responses, containing (in mM): K-gluconate, 135; EGTA, 1.0; HEPES, 10; $CaCl_2$, 0.1; $MgCl_2$, 2; Mg-ATP, 2; pH = 7.3. After addition of 5 mg/mL biocytin, the osmolarity of the solution was adjusted to between 270 and 280 mOsm. The resistance of the pipettes was 4–10 MΩ and the reverse potential of $GABA_A$ currents was ≈ –60 mV. Synaptic currents were acquired using Digidata 1200B (Axon Instruments) acquisition card. Data were analysed using Acquis1 software (Gérard Sadoc, Gif/Yvette, France). Capacitance values were determined by curve fitting of the capacitive current generated by a 5-mV depolarizing voltage step. Identification of evoked responses was made using specific receptor antagonists: 6-cyano-7-nitro quinoxaline-2,3-dione (CNQX), D-APV and bicuculline.

Morphological reconstructions

Recordings with biocytin-filled electrodes were usually made from a single cell in each slice. More than one cell labelled per slice was occasionally patched, but in two distinct CA1 areas. After recording, the patching electrode was slowly removed from the cell and the slice was fixed overnight at 4 °C in a solution of 4% fresh paraformaldehyde and 0.2% glutaraldehyde in 0.1 M phosphate buffer and then left for at least 24 h in a 30% sucrose solution containing 0.1% NaN_3 in 0.1 M phosphate buffer. For some slices a cresyl violet staining was also performed for a better identification of the limits of CA1 layers. Neurons were then visualized using the avidin-biotinylated horseradish peroxidase complex reaction (Vestastin Elite ABC kit, Vector Laboratory, Burlingame, CA, USA) using 3,3′-diaminobenzidine (DAB) as chromogen. Slices were rinsed for 30 min in 0.05 M Tris-buffered saline (TBS) at pH = 7.4 containing 0.3% Triton X-100 and incubated overnight at 4 °C with the avidin–biotin–peroxidase solution. Slices were washed for 30 min with TBS and rinsed for 10 min with Tris buffer (TB) at pH = 7.6, and then processed for 15 min in 0.06% DAB tetrahydrochloride and 0.01% hydrogen peroxide, diluted in TB. They were then rinsed for 30 min in TB, mounted on gelatin-coated slides, dehydrated and cover-slipped with Permount (Fischer Scientific, Euromedex, France). Reconstruction of dendritic and axonal arborization of stained cells was performed using a camera lucida and a Leitz Orthoplan microscope with a 40× oil-immersion objective. This was made in a double-blind procedure by an experimenter unaware of the physiological data. Dendritic and axonal processes were followed either to their termination or to the point where they left the slice. Graphs were digitized and converted to high-resolution black-and-white bitmap files. The number of black pixels was then determined using homemade software (S-Neuron).

Immunocytochemistry

After transcardial perfusion of newborn P0 rats with paraformaldehyde (4%) and glutaraldehyde (0.2%), brains were kept overnight in 4% paraformaldehyde. Vibratome 40-μm-thick sections were incubated overnight with primary antibodies (see below) in PBS containing 5% normal goat serum. After washing, sections were sequentially incubated with biotinylated antirabbit antibody (1 : 400; Vector Laboratories) and avidin–biotin–peroxydase solution (Vectastain Elite ABC, Vector Laboratories). Sections were then processed in DAB tetrahydrochloride (0.06%) and hydrogen peroxyde (0.01%) and then rinsed, dehydrated and mounted with Permount. Adjacent sections were incubated in the absence of either primary or secondary antibodies to check the specificity of the peroxidase staining. Non-specific staining was prevented by pre-incubating the sections with gelatine (0.5%) and normal goat serum (10%) (Vector Laboratories). Primary antibodies for indirect immunohistochemistry included polyclonal rabbit antiparvalbumin (PV; 1 : 5000; Swant, Switzerland), somatostatin (SOM, Peninsula Labs, CA USA; 1 : 200), calbindin D-28K (CB; 1 : 10 000; Swant); and calretinin (CR; 1 : 2000; Swant).

Drugs

Bicuculline methochloride, CNQX, D-APV, isoguvacine, S-AMPA and NMDA were purchased from Tocris Neuramin (UK). TTX was from Latoxan (France), biocytin, 4-aminopyridine (4-AP), α-latrotoxin and other chemicals were purchased from Sigma (France).

Statistical analysis

Data are expressed as mean ± SEM. Statistical significance of differences between means was assessed using unpaired two-tailed *t*-test. The level of significance was set at $P < 0.05$.

Results

Intrinsic interneurons

The present results are based on patch-clamp recordings from 162 interneurons located in the CA1 area of P0 slices. All interneurons were filled with biocytin through the patch pipette and reconstructed *post hoc* and a quantitative analysis of the morphological parameters was performed. In addition, in foetal slices (E18–20), 69 interneurons and 52 pyramidal cells were recorded in parallel.

Sequential expression of GABA and glutamatergic synapses at P0

In the first part of this study, 131 interneurons were patched blindly in all CA1 areas of the hippocampus at P0. Depending on their spontaneous and evoked postsynaptic currents (PSCs) as well as their morphological reconstruction, interneurons can be classified into three types:

Non-innervated 'silent' interneurons

These represent 4.6% (six cells) of the analysed population of interneurons at P0. They were identified as neurons (vs. glia) by the TTX-sensitive inward sodium spikes evoked by depolarizing steps (30 mV, from –60 mV; Fig. 1A). When recorded over 30–60 min, they had no spontaneous PSCs and repetitive electrical stimulation of afferent fibres at high intensity (70–90 V) and frequency (100 Hz, 1 s) did not evoke PSCs (Fig. 1B). No response was observed, either, upon application of 4-AP (100 μM; see below) for >1 h. Finally, there was also no action current in long-lasting cell-attached recordings (not shown). These neurons have, however, ionotropic GABA and glutamate receptors as, in the presence of TTX (1 μM), bath application of isoguvacine (0.7 μM, 1 min) or AMPA (5 μM, 1.5 min) generated small inward currents (25 ± 4 pA, $n = 3$ and 31 ± 5 pA, $n = 3$, respectively) which were blocked by bicuculline (10 μM) and CNQX (10 μM, 10 min), respectively. At +40 mV, NMDA (10 μM, 3 min) also gave rise to a small current (11 ± 2 pA, $n = 3$) which was blocked by D-APV (20 μM; data not shown). Therefore, $GABA_A$ and glutamate receptors were expressed before corresponding synapses. Non-innervated neurons (cells 1–6, Fig. 1C) were observed in SR ($n = 4$), in the vicinity of the pyramidal layer ($n = 1$) and at the border with SLM ($n = 1$). These neurons had a total surface area (calculated automatically, with the Neurolucida program of Microbright Fields, USA) of 187 ± 6 μm^2, with a small soma (84 ± 11 μm^2), and their axons (16 ± 2 μm^2) and dendrites (88 ± 13 μm^2) were poorly developed and remained in SR.

Interneurons with GABA but not glutamate PSCs (G interneurons)

These constituted 16.8% (22 cells) of the population of interneurons. In these neurons, only spontaneous and evoked GABAergic PSCs were recorded during at least 60 min. Large spontaneous currents, reminiscent of GDPs, were occasionally observed but were consistently evoked by electrical stimulation (Fig. 2A). Bath application of bicuculline (10 μM, 10 min) fully blocked the PSCs and GDP-like events. Strong stimuli at various membrane potentials failed to evoke glutamate-mediated PSCs (Fig. 2A). Furthermore, no spontaneous or evoked epileptic discharges were observed upon application of bicuculline for 30 min ($n = 8$). G interneurons (cells 7–28; Fig. 2B), which were clearly more developed than non-innervated interneurons (see below), were found in all CA1 layers but not in SLM. They were morphologically heterogeneous with short dendrites and axons with generally no collaterals. G interneurons from SR could be divided into two categories, one having an axon that remained strictly in SR and one that constituted a homogeneous population of stellate cells, located close to the pyramidal cell layer (cells 15–22) with a unique axon that entered SP (Fig. 2B).

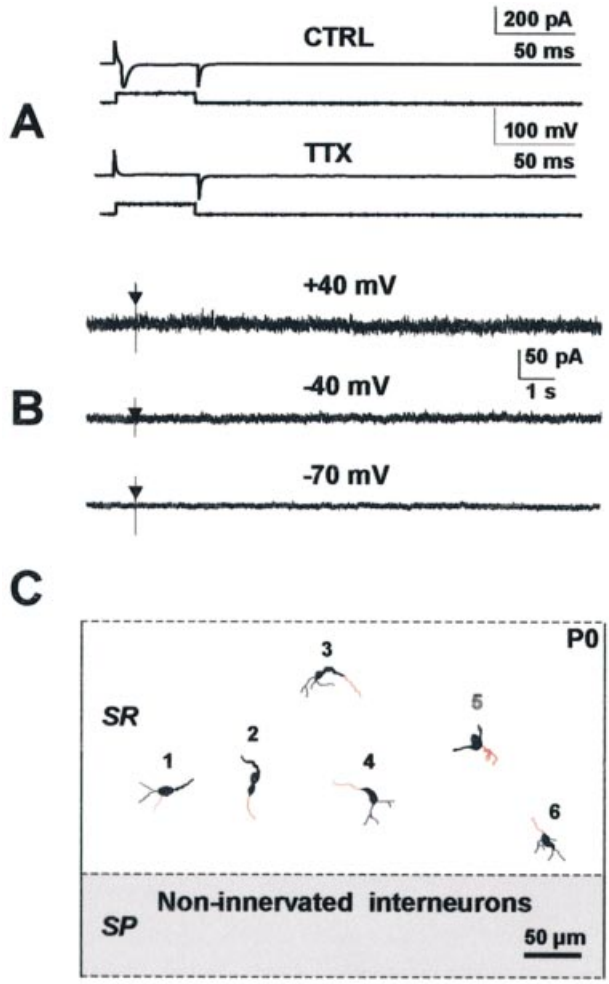

FIG. 1. Morphofunctional characteristics of non-innervated CA1 interneurons at P0. (A) The fast inward Na^+ current evoked by a 30-mV depolarizing step for 50 ms was blocked by bath application of TTX (1 μM). (B) No spontaneous or evoked activity (arrow, 80 V, 60 μs duration) could be recorded at three different membrane potentials. (C) Reconstructed non-innervated interneurons filled with biocytin (cells 1–6) were all located in SR.

Interneurons with GABA and glutamate PSCs (GG interneurons)

These represented the majority of CA1 interneurons at P0 (78.6%, 103 cells). In addition to currents corresponding to GDPs, spontaneous and evoked PSCs mediated by $GABA_A$, AMPA and NMDA receptors were usually recorded in the first 2–5 min (Fig. 3). Thus, at –45 mV, bicuculline blocked GABAergic outward currents and induced spontaneous and evoked interictal responses. The remaining spontaneous and the large evoked inward responses (Fig. 3B) were abolished by CNQX (10 μM, 10 min; Fig. 3C). At +40 mV, the

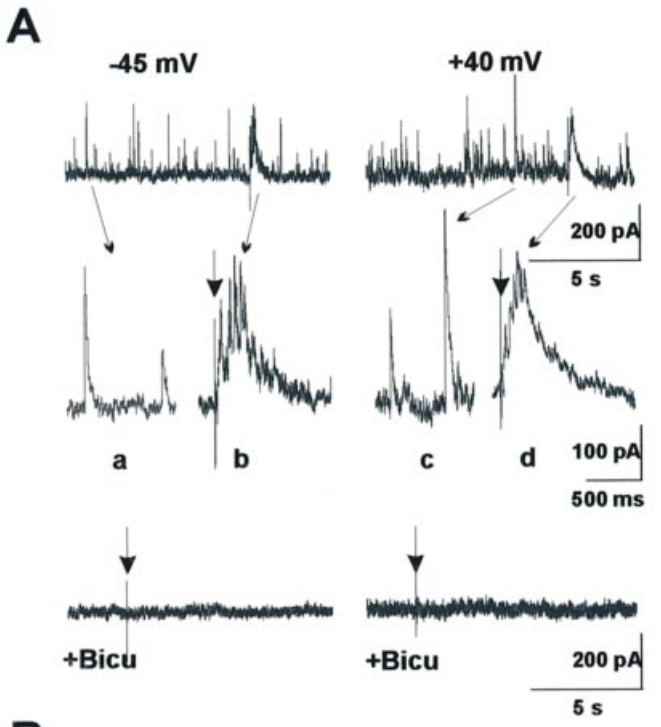

FIG. 2. Morphofunctional characteristics of G interneurons at P0. (A) Spontaneous and evoked outward PSCs mediated by $GABA_A$ receptors were recorded in SR at –45 and at +40 mV with K-gluconate-filled electrodes (the reversal potential for $GABA_A$ currents was –61 mV); (a–d) enlargements showing isolated PSCs and the GDP-like evoked responses. Application of bicuculline (10 µM, 10 min) completely suppressed spontaneous and evoked (arrow, 80 V, 60 µs) $GABA_A$ responses at the two potentials. Note the absence of interictal seizures and that no NMDA response was evoked at +40 mV in these conditions. (B) Morphology of 22 G interneurons at P0. G interneurons were reconstructed and represented in their layers. Arrows indicate where axons are leaving the slice. Note that cells 15–22 are located at the border with SP. They have a stellate morphology and their axons invade SP.

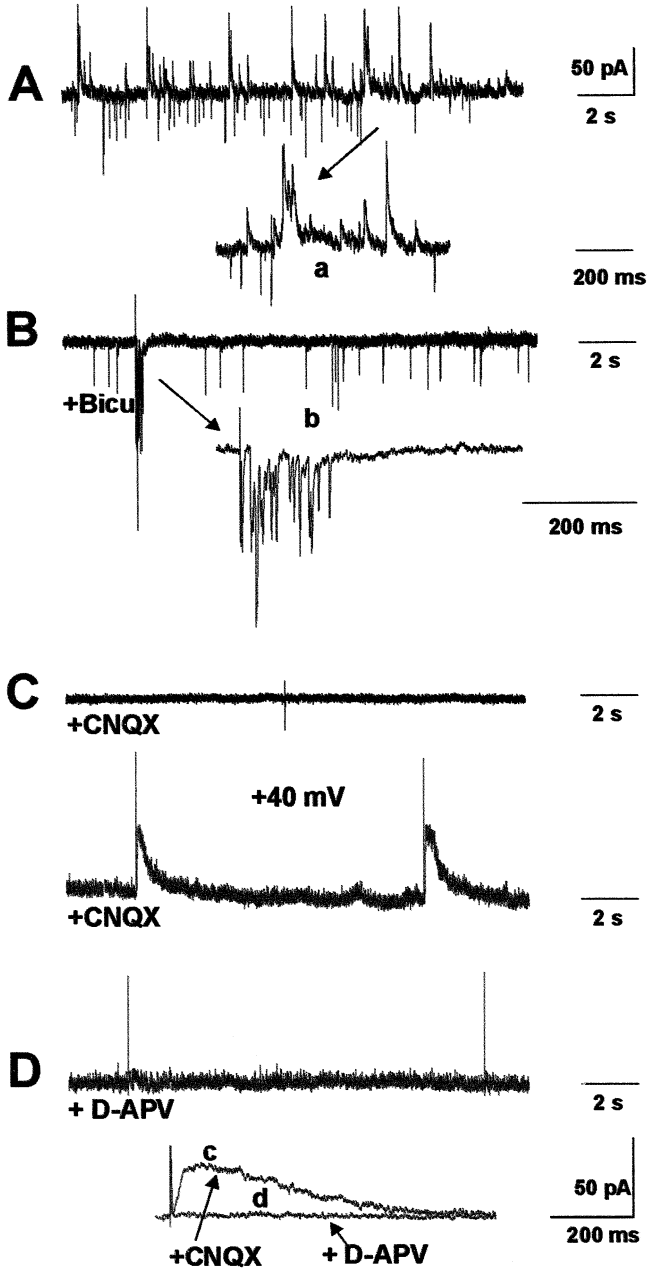

FIG. 3. Electrophysiological characteristics of GG interneurons at P0. (A) spontaneous and evoked $GABA_A$ (outward) and AMPA (inward) PSCs were recorded at –45 mV in K-gluconate-filled electrodes (reversal potential for $GABA_A$ currents was ≈–59 mV). Outward GDPs were present in this record; (a) the enlargement illustrates the different kinetics of the two types of PSCs. (B) Application of bicuculline (10 µM, 10 min) completely suppressed outward but not inward spontaneous or evoked currents; (b) enlargement of the interictal-like evoked response. (C) Addition of CNQX (10 µM, 10 min) to bicuculline suppressed AMPA receptor-mediated spontaneous and evoked currents at –45 mV. (D) In the presence of AMPA and $GABA_A$ receptor antagonists, large evoked and spontaneous outward currents were recorded at +40 mV. They were abolished by concomitant addition of D-APV (20 µM, 10 min); (c and d) mean of three evoked responses obtained in the presence of bicuculine and CNQX, before and after addition of D-APV (20 µM, 10 min).

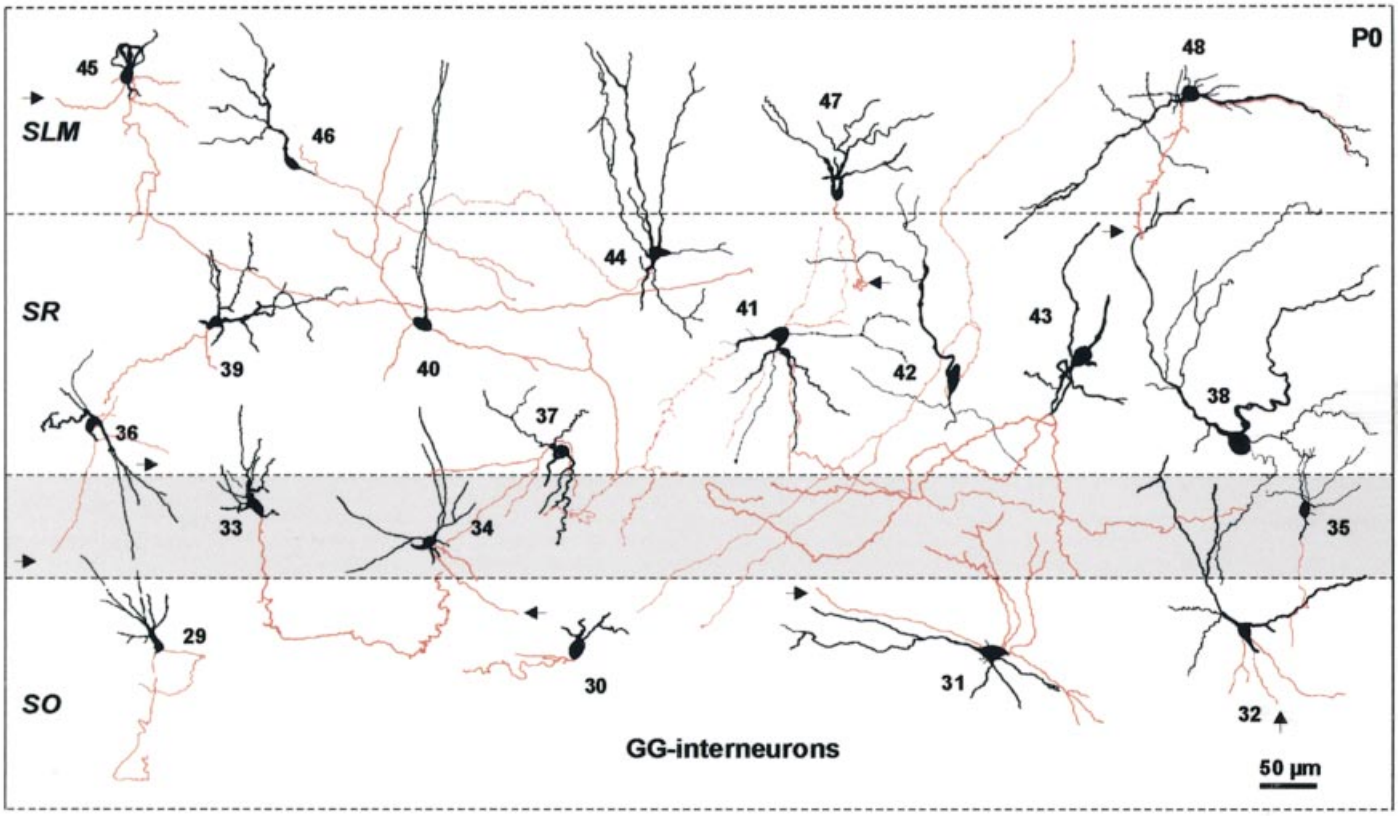

FIG. 4. Morphology of GG interneurons at P0. Twenty of the 103 GG interneurons are represented, illustrating their morphological heterogeneity. Arrows indicate where axons are leaving the slice. Their size, axonal arbor and dendritic trees are different from cell to cell. Four of them were in SO (cells 29–32) and cells 33–35 represent three examples of GG interneurons located in SP with their axons extending to SO. Cells 36–44 are located in SR. Cell 39 is an example of an interneuron with dendrites and axon that remain in SR. Cells 36–38 and 40–43 correspond to bistratified cells with dendrites in SR and either SP (36 and 37) or SLM (38, 40, 42 and 44). In addition, cell 37 is an example of a stellate interneuron located at the border with SP. The axons of neuron 42 invaded both SO and SLM. In SLM, cells 45, 46 and 47 send their axons into SR. They are parallel, oblique or perpendicular to SLM. Neuron 48 may correspond to a horizontal bipolar cell.

current remaining after CNQX application was subsequently blocked by D-APV (20 µM; Fig. 3D). During this analysis we also noted that the voltage-dependence of AMPA PSCs displayed a rectification at positive voltages that has not previously been observed in pyramidal cells (Tyzio *et al*., 1999), suggesting that, in interneurons, AMPA receptors may be calcium-permeable. In addition, none of the neurons recorded expressed NMDA but not AMPA PSCs.

GG interneurons have very heterogeneous shapes with round, oval, fusiform and pyramidal somata. Some of them are illustrated in Fig. 4 (cells 29–48). They were more frequently recorded in SR ($n = 64$) and were also found in all CA1 layers (SO, $n = 8$; SP, $n = 10$; SLM, $n = 21$). GG interneurons from SR with radial dendrites (29 cells) were more frequently encountered than cells with horizontal dendrites (10 cells), the dendrites of the others (26 cells) extended in the two directions. This suggested that GG interneurons probably received their glutamatergic inputs from Schaffer and commissural fibres. The majority of GG interneurons from SR had dendrites which remained strictly in SR, but some cells were bistratified (SR and SP or SR and SLM) or their dendrites were found in three different layers (SR, SP and SLM, or SR, SP and SO). The axons of the majority of GG interneurons from SR also remained in SR (28 cells). Axons from other cells reached SP (18 cells) and SLM (eight cells) and a few others were also found in two (SP and SO: six cells; SP and SLM: one cell) or three distinct CA1 areas (three cells). In spite of this morphological diversity, functional glutamatergic synapses were found in interneurons with axonal and dendritic arbors that were clearly more developed than those of G interneurons.

Quantitative morphofunctional analysis

This study was based on the measurement of the cell body surface, the dendritic and axonal arbor and the total surface of the neuron as well as its capacitance. Neuronal reconstructions made with a camera lucida did not allow precise determination of 3-D characteristics. Furthermore, it was obvious that some axons had been cut by the slicing procedure, minimizing the values for GG interneurons particularly. In spite of these limitations, we were generally able to follow most processes within the thickness of the slice, probably because of the relatively small size of the neurons. Quantitative examination of the morphological features of the three populations of neurons (131 cells) confirmed that they correspond to three different developmental degrees (Fig. 5). G interneurons were clearly more developed than non-innervated interneurons and less developed than GG interneurons, and this general observation was valid whatever the location of the neurons. Thus, G interneurons had a significantly greater surface area than non-innervated cells ($P < 0.0001$) but a smaller surface than GG interneurons ($P < 0.0001$) (Fig. 5A). In addition, the surface areas of axons and dendrites of G interneurons were also significantly greater than those of non-innervated cells ($P < 0.0001$ and $P < 0.0001$, respectively) but smaller than those of GG interneurons ($P < 0.0001$ and $P < 0.0001$, respectively)

(Fig. 5B). In contrast, although larger than non-innervated cells, the surface areas of somata of G and GG interneurons were not significantly different ($P = 0.6862$), suggesting that the size of the cell body reaches a plateau when GABAergic synapses are functional (Fig. 5B).

The capacitance of G interneurons (27.3 ± 0.6 pF, $n = 22$) was significantly higher ($P < 0.0001$) than that of non-innervated neurons (18.7 ± 0.7 pF, $n = 6$) and significantly smaller ($P < 0.0001$) than that of GG interneurons (41.4 ± 0.9 pF, $n = 103$). Likewise, in all CA1 areas the highest capacitance values were associated with GG interneurons whereas G interneurons and non-innervated cells displayed significantly lower values (Fig. 5C). The capacitance of all 131 interneurons correlated ($r = 0.896$) with their surface (Fig. 5D) and the extent of arborization. Therefore, non-innervated, G-only and GG interneurons correspond to three developmental degrees but the question of a linear or step-by-step development remains to be investigated. Nevertheless, the capacitance and other morphological variables enable prediction of whether an interneuron will have functional synapses, in spite of the heterogeneity of interneurons. This was confirmed using visual patch.

Visual patch recordings

In the second part of this study we recorded, at P0, 31 additional interneurons under visual control.

Non-innervated cells

Blind patch studies indicated that small P0 interneurons had no synapses. However, as our sample of non-innervated 'silent' interneurons was limited to six cells, we used the visual infrared technique to select under visual control small P0 interneurons from SR (10 cells) and SO (nine cells). Stimulation was performed in both SR and SO. In seven neurons from SR and in six neurons from SO, no spontaneous or evoked PSCs could be observed, the other neurons being of the G-only type and morphologically more developed. It was also important to verify that the lack of synaptic responses in non-innervated neurons was not due to synapses that rarely release transmitters spontaneously or that are difficult to activate with a stimulating electrode. We therefore bath-applied 4-AP (100 μM), a K^+-channel blocker (Storm, 1988) that augments transmitter release (Pena & Tapia, 1999; Perreault & Avoli, 1991). In P0 slices, 4-AP (100 μM, 60 min) did not generate any spontaneous or evoked PSCs in non-innervated interneurons from SR ($n = 6$) (Fig. 6A). Furthermore, no current was detected during 15–30 min in additional non-innervated interneurons ($n = 3$) perfused with α-latrotoxin (0.6 nM, 1 min), which depletes vesicular pools (Fig. 6A; Sudhof, 2001). Therefore, small interneurons had no functional synapses.

G interneurons

Blind patch recordings have also suggested that G interneurons are preferentially located in the immediate vicinity of the pyramidal layer

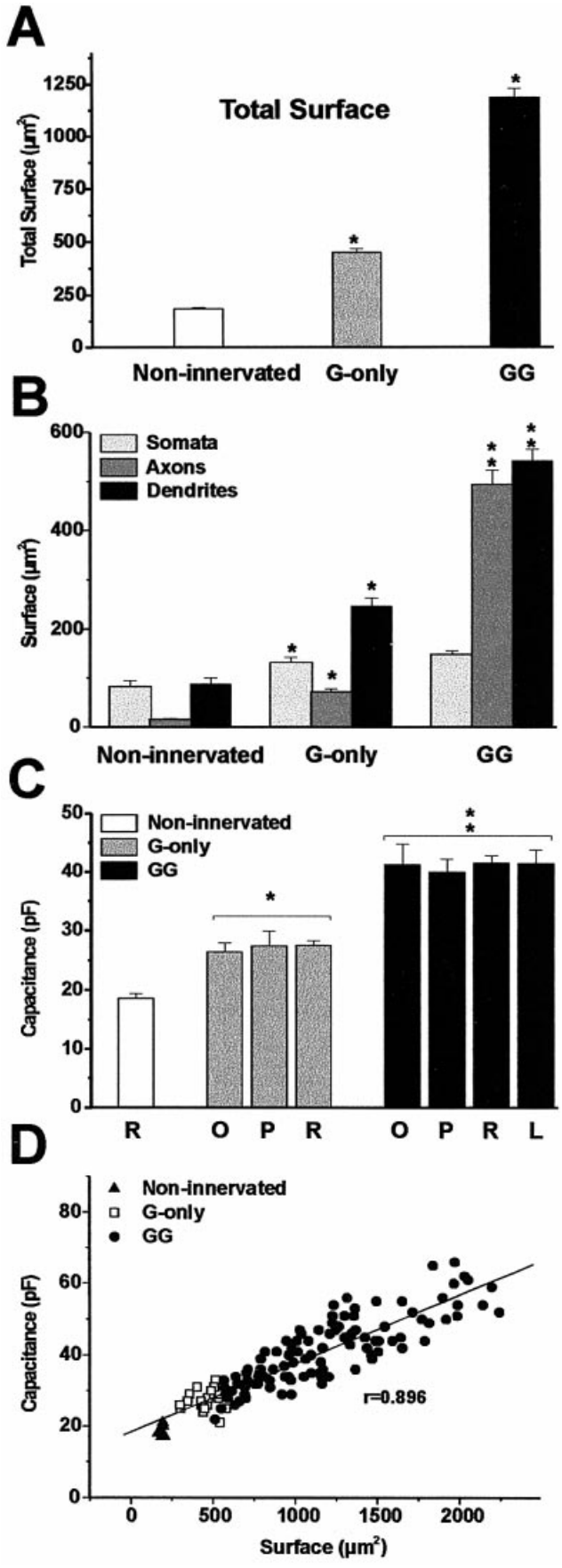

FIG. 5. Quantitative morphological characteristics of 131 interneurons at P0. (A) Representation of the mean total surface of non-innervated (six cells), G-only (22 cells) and GG interneurons (103 cells). (B) Mean of respective surface of somata, axons and dendrites of non-innervated G-only and GG interneurons. (C) The capacitance of non-innervated G-only and GG interneurons are reported according to their respective location in CA1 layers (O, P, R and L correspond to SO, SP, SR and SLM, respectively). *$P < 0.05$ for noninnervated vs. G-only or GG interneurons; **$P < 0.05$ for GG vs. G interneurons. (D) Correlation between the total surface area of 131 CA1 interneurons and their respective capacitance; 'r' is the coefficient of the linear correlation plotted.

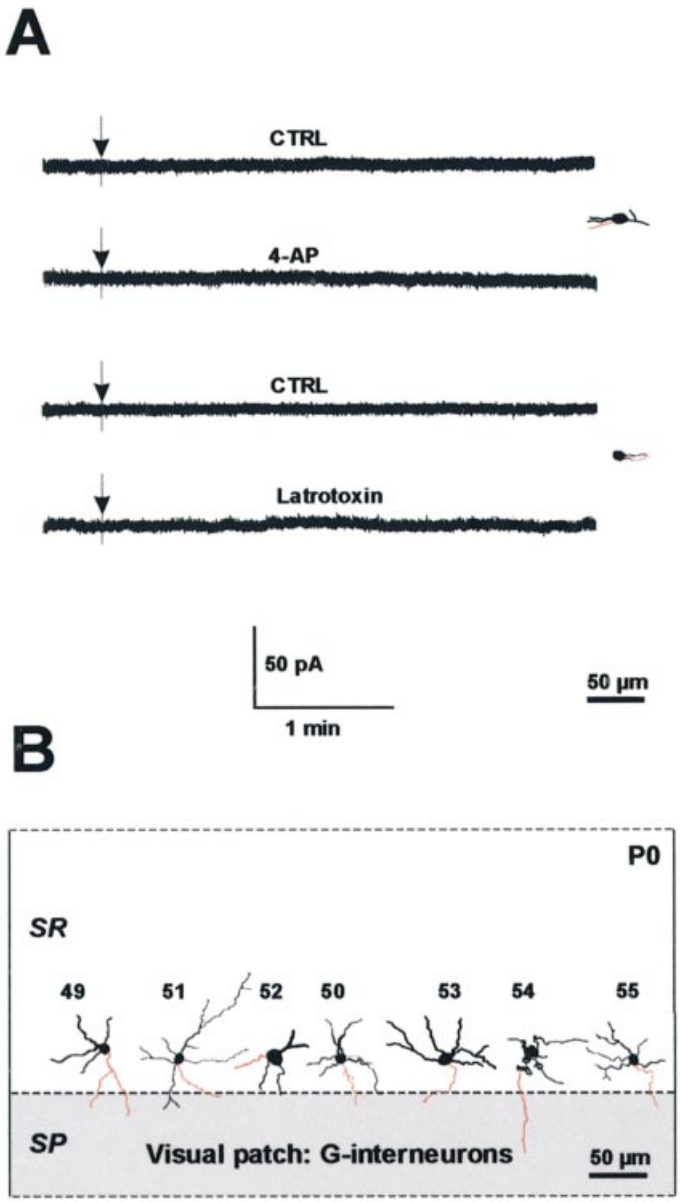

FIG. 6. CA1 cells recorded under visual control at P0. (A) Non-innervated interneurons remained 'silent' even if the release of neurotransmitter was increased by 4-AP or by α-latrotoxin. Small interneurons from SR selected under visual guidance were found to have no spontaneous or evoked (arrow, 80 V, 60 µs) synaptic responses in control conditions (CTRL) or 30 min after application of 4-AP (100 µM, 30 min) or α-latrotoxin (0.6 nM, 1 min). An example of the morphology of these cells is represented. (B) Cells located at the border of the pyramidal layer were selected (48–54) and recorded. They were found to correspond to G interneurons with a stellate morphology, with their axons generally entering SP.

(64% of G interneurons and 40% of all interneurons are located in SR). This location was surprising but visual patch recordings confirmed that this was not the result of a bias of the blind patch technique because seven out of 12 interneurons (58%) patched under visual guidance in this region (cells 49–55; Fig. 6B) had only GABA PSCs. These neurons had stellate type morphology and a surface area (448 ± 26 µm^2, n = 7) which was similar to that of blind patch-recorded G interneurons in the same area (482 ± 27 µm^2, n = 9). The five other interneurons (42%) corresponded to GG interneurons and were clearly morphologically more developed. Finally, as expected, large interneurons recorded under visual guidance in SR corresponded to GG interneurons and the mean of their surface area (1075 ± 103 µm^2, n = 6) was not significantly different from that of blindly patched GG interneurons (1183 ± 52, n = 64).

Immunocytochemistry in P0 slices

In addition to their morphology and functional responses, interneurons have been identified by their content of peptides (Freund & Buzsáki, 1996). In this study, we have performed an immunocytochemical detection of some peptides to examine whether it was possible to recognize at P0 the morphology of more mature functional interneurons (data not shown). Briefly, slices were stained with calbindin (CB), somatostatin (SOM) and calretinin (CR) but not with parvalbumin (PV) polyclonal antibodies (data not shown). Briefly, CB immunoreactivity was observed in the hippocampus of newborn rats as previously reported (Super & Soriano, 1994). In SO (the more intensely stained) and SR, cell bodies and small thin dendrites were immunoreactive. A few pyramidal cells were also stained; the cell body and the apical dendrite contained within SP were lightly immunoreactive. As reported for adults (Blasco-Ibanez & Freund, 1995; Katona *et al*., 1999), SOM-positive cells were observed in the SO and only few axons were immunoreactive in SLM. CR immunoreactivity was intense in SLM of P0 rats, reflecting the presence in this layer of Cajal–Retzius cells. In addition, scattered small neurons were immunoreactive in the SO, SP and SR, as previously reported (Jiang & Swann, 1997). No PV-immunoreactive cells were observed in P0 hippocampal sections, in agreement with other investigators (Nitsch *et al*., 1990; Solbach & Celio, 1991), whereas as positive control, cells were immunoreactive to the same antibody in P7 rats (not shown).

Sequential formation of synapses in foetal interneurons

Our results suggest that there is a developmental program in both interneurons and pyramidal cells (Tyzio *et al*., 1999) but that the interneuronal network may mature at an earlier stage. Indeed, at P0, 78% of interneurons but only 8% of pyramidal neurons express GABAergic and glutamatergic synapses. Conversely, 79% of pyramidal neurons but only 5% of interneurons were not innervated at this developmental stage (Fig. 7A). We next determined whether this template is also valid at an earlier developmental stage. Because the activity of pyramidal neurons *in utero* has not been determined in previous studies, we recorded in foetal slices (E18–20) both pyramidal neurons and interneurons. Pyramidal neurons *in utero* have a similar sequence of development but the majority of neurons are nonfunctional. Thus, 88% of pyramidal neurons (46 out of 52) had no spontaneous or evoked PSCs with only 6% of neurons having both $GABA_A$ and glutamate PSCs (three cells). In contrast, 65% of interneurons (45 out of 69) recorded in the same slices had functional synapses (37.6% of G interneurons, n = 26; and 27.5% of GG interneurons, n = 19 cells; Fig. 7B). These observations suggest that interneurons are in a more advanced developmental stage than pyramidal cells *in utero*. They also extend the conclusion that GABA synapses are formed before glutamate ones as the ratio of G : GG interneurons was more than six times higher at E18–20 (1.36) than at P0 (0.21).

Long-range projections of interneurons

In addition to the 162 CA1 interneurons described above that remained in the CA1 area, we also recorded 12 interneurons (Fig. 8) that displayed $GABA_A$, AMPA and NMDA receptor-mediated currents but with arborization not restricted to the CA1 area. Five

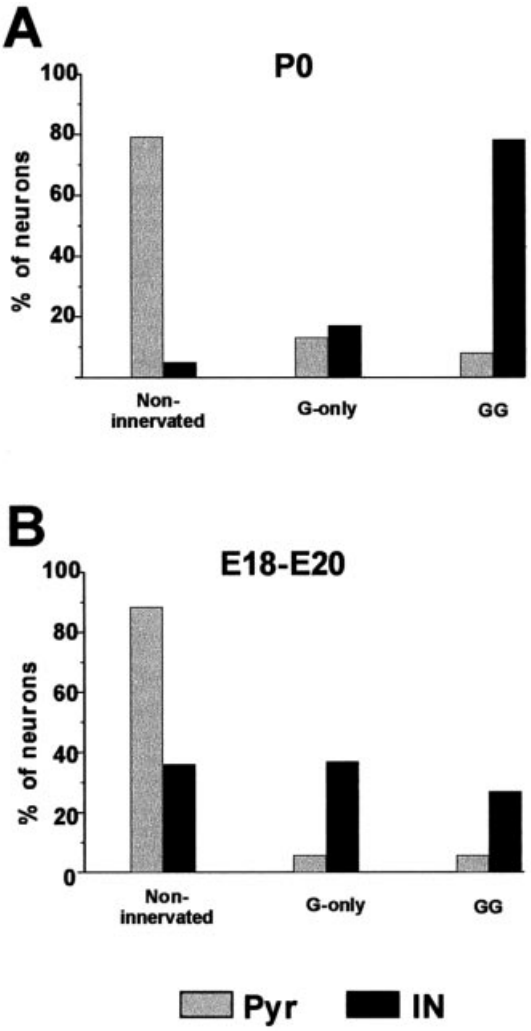

FIG. 7. Relative proportions of the three types of pyramidal cells (data from Tyzio *et al.*, 1999) and interneurons (131 cells) at two developmental stages. (A) At P0, 78% of the interneurons are functional whereas 78% of the 59 pyramidal cells are nonfunctional. (B) In embryonic slices, beside pyramidal cells (52 cells) that are mainly (88%) non-innervated, a large proportion (65%) of interneurons are already functional (45 out of 69 cells). Pyr, pyramidal cells; IN, interneurons.

neurons projected their axons to the CA3 region and their cell bodies were in SP (55), SR (cells 56 and 57), SLM (cell 58) and SO (cell 59), respectively. They resemble back-projection, horizontal and oriens lacunosum moleculare (O-LM) neurons, respectively, which have been reported in adults but with much less developed axonal and dendritic trees. The axons of interneurons 55 and 56 invaded SR of CA3 and reached the border of the pyramidal layer. However, the hilus was not crossed by these axons. Three interneurons (57, 58 and 59) were less developed but also reached the SLM of CA3. The axons of three interneurons (60, 61 and 62) were directed towards the subiculum. Two of them (cells 61 and 62) were located in SLM of CA1 and the dendrites of one interneuron (cell 62) crossed the fissure to enter the granular layer of the dentate gyrus. Four other interneurons (63–66) also crossed the fissure but did not enter the granular layer or the hilus. Thus, the axons of interneurons 63 and 64 were found at the limit of granular cells, whereas it was the dendritic tree of cells 65 and 66 which reached this region. Interestingly, cell 66 displays several morphological characteristics of a perisomatic cell but its axonal arbor was poorly developed and did not enter the pyramidal layer of CA1.

Discussion

The results of our study suggest that there is a developmental program of synapse formation with the sequential establishment of $GABA_A$ synapses prior to glutamatergic ones occurring first in interneurons then in pyramidal neurons (summarized in Fig. 9). In foetal slices the first functional synapses are GABAergic synapses established between interneurons. As a consequence, the interneuronal network is already operative through excitatory $GABA_A$ synapses at a time when most principal cells are quiescent with no synaptic connections. Our results provide a general frame for the maturation of a cortical network and suggest that the consequence of these developmental gradients is that interneurons are in a position to exert a key role in the early maturation of the hippocampal network.

Interneurons are functionally mature before pyramidal cells

At P0, interneurons are morphologically heterogeneous but can be classified into three stages of functional development: non-innervated interneurons with no synapses, G interneurons with $GABA_A$ synapses only and GG interneurons with $GABA_A$, AMPA and NMDA synapses. A similar heterogeneity has been reported in pyramidal cells (Tyzio *et al.*, 1999) but, at the same age, the proportion of the three developmental stages dramatically differs. At P0, the majority of interneurons (78%) but only 8% of pyramidal cells correspond to GG neurons. Conversely, 79% of pyramidal cells but only 5% of interneurons are non-innervated at P0. We extended this observation to foetal neurons (E18–20) where 88% of pyramidal neurons are non-innervated whereas 65% of interneurons are already functional. At an early stage, the functional activity resulted mainly from the activation of interneurons suggesting that the field potential previously recorded *in utero* in intact hippocampi (Diabira *et al.*, 1999) is probably due to the activation of glutamatergic synapses on interneurons. This is in keeping with the observation that interneurons divide prior to pyramidal neurons (Soriano *et al.*, 1986; Altman & Bayer, 1990).

Interestingly, we have previously reported that a small percentage (2%) of pyramidal neurons have $GABA_A$ and NMDA, but not AMPA, receptor-mediated synapses (Tyzio *et al.*, 1999), but in this study we failed to identify such silent glutamatergic synapses in interneurons using the same approach. This failure is unlikely to be due to a sampling problem as glutamatergic synapses are 10× more frequent in interneurons than in pyramidal cells. Minimal stimulations should be used to confirm this observation, which may suggest that the hypothesis of silent glutamatergic synapses, with NMDA but not AMPA synapses, may not be valid for interneurons.

Morphofunctional sequential formation of $GABA_A$ and glutamatergic synapses

In CA1 interneurons, $GABA_A$ synapses appeared before glutamatergic synapses as none of the recorded embryonic and P0 interneurons expresses glutamatergic but no $GABA_A$ synapses. In addition, the majority of functional interneurons in embryonic slices were G-only interneurons whereas the proportion of GG interneurons dramatically increased at P0 with a simultaneous reduction of G-only interneurons. The same sequence of synapse formation was reported in pyramidal cells from rat (Tyzio *et al.*, 1999) or macaque (Khazipov *et al.*, 2001) hippocampus. Electrophysiological observations also report that $GABA_A$ synapses appear before AMPA synapses in rat neocortex (Owens *et al.*, 1999) and isolated rat spinal cord (Nishimaru *et al.*,

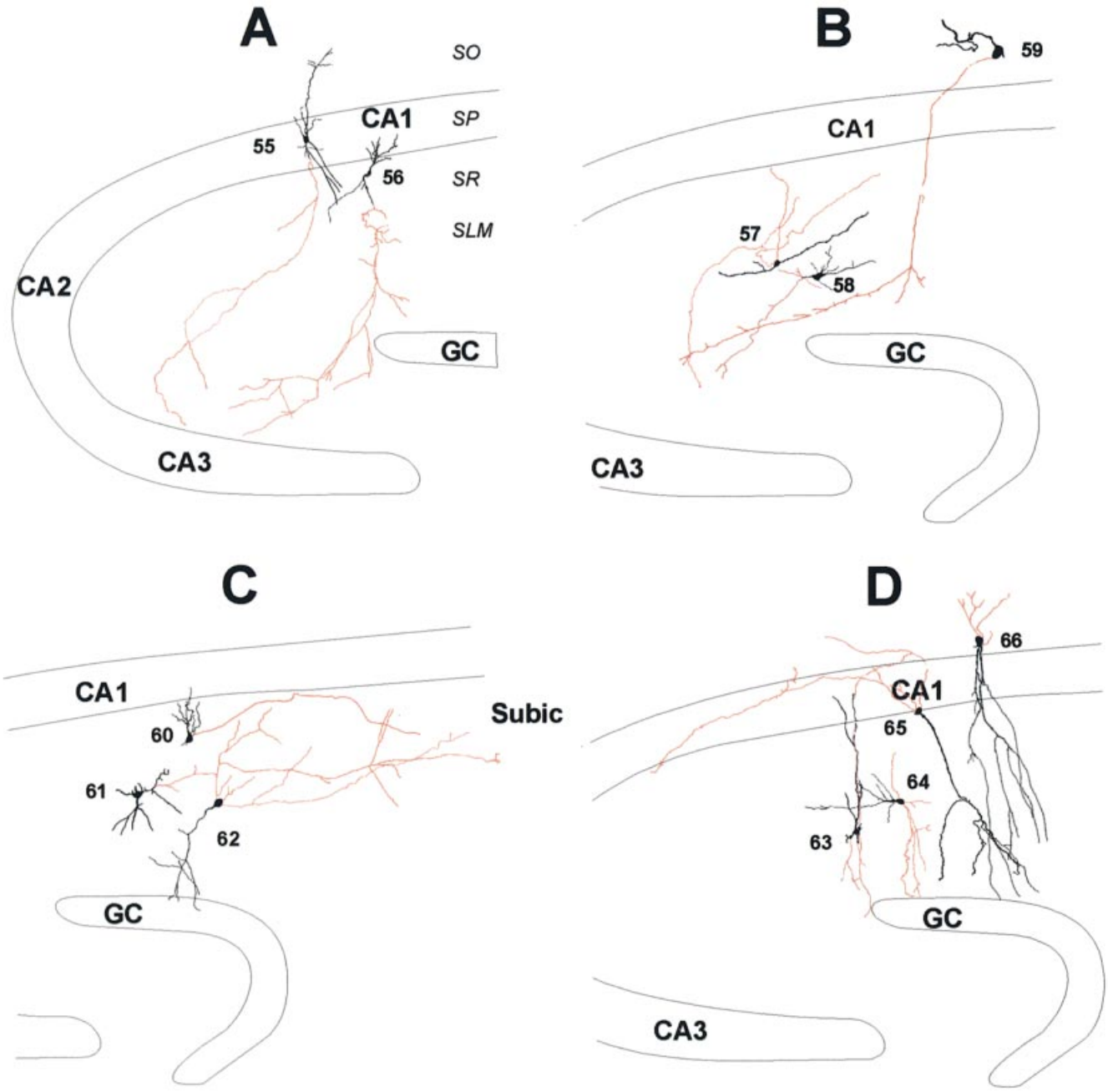

FIG. 8. GG interneurons extending their axonal or dendritic arbors outside the CA1 area. Reconstruction of biocytin-filled interneurons at P0. Only pyramidal layers and granular cells are represented. (A,B) The axons of these interneurons invade the CA3 area. Their somata are located in all CA1 layers. (C) The axons of these interneurons project towards the subiculum (Subic). They have distinct morphology and their somata are located in SR or SLM. Note that the dendrites of neuron 62 cross the fissure and reach the granular cell layer. (D) Examples of interneurons which also reach the fissure but whose axons or dendrites do not invade the granular cell layer.

1996), suggesting that this is a general property of developing neurons that has been kept across evolution from rodents to primates. In addition, $GABA_A$ receptors were also detected before glutamatergic receptors by application of specific agonists in rat embryonic spinal cord cells (Walton *et al*., 1993) and in cell cultures from rat hypothalamus (Chen *et al*., 1995), hippocampus, septum and neocortex (Koller *et al*., 1990), suggesting that even extrasynaptic receptors follows the same developmental sequence. This sequential formation of synapses is correlated with different morphological features. Indeed, $GABA_A$ synapses were observed in interneurons with poorly developed dendrites, whereas glutamatergic synapses were found on interneurons with much longer dendrites and axons. Therefore, the functional state of a developing interneuron can be predicted by examining its morphological features.

The delayed formation of glutamatergic synapses cannot be ascribed to a delayed distribution of the corresponding afferent fibres as intrinsic and extrinsic afferent fibres are already present at P0 in several CA1 layers (SO, SR, SLM) of the rat (Diabira *et al*., 1999) and mouse (Super & Soriano, 1994) hippocampus. Therefore, in spite of these multiple excitatory inputs, GABAergic but not glutamatergic synapses were first established in immature neurons, suggesting that the availability of excitatory inputs is necessary but not sufficient for

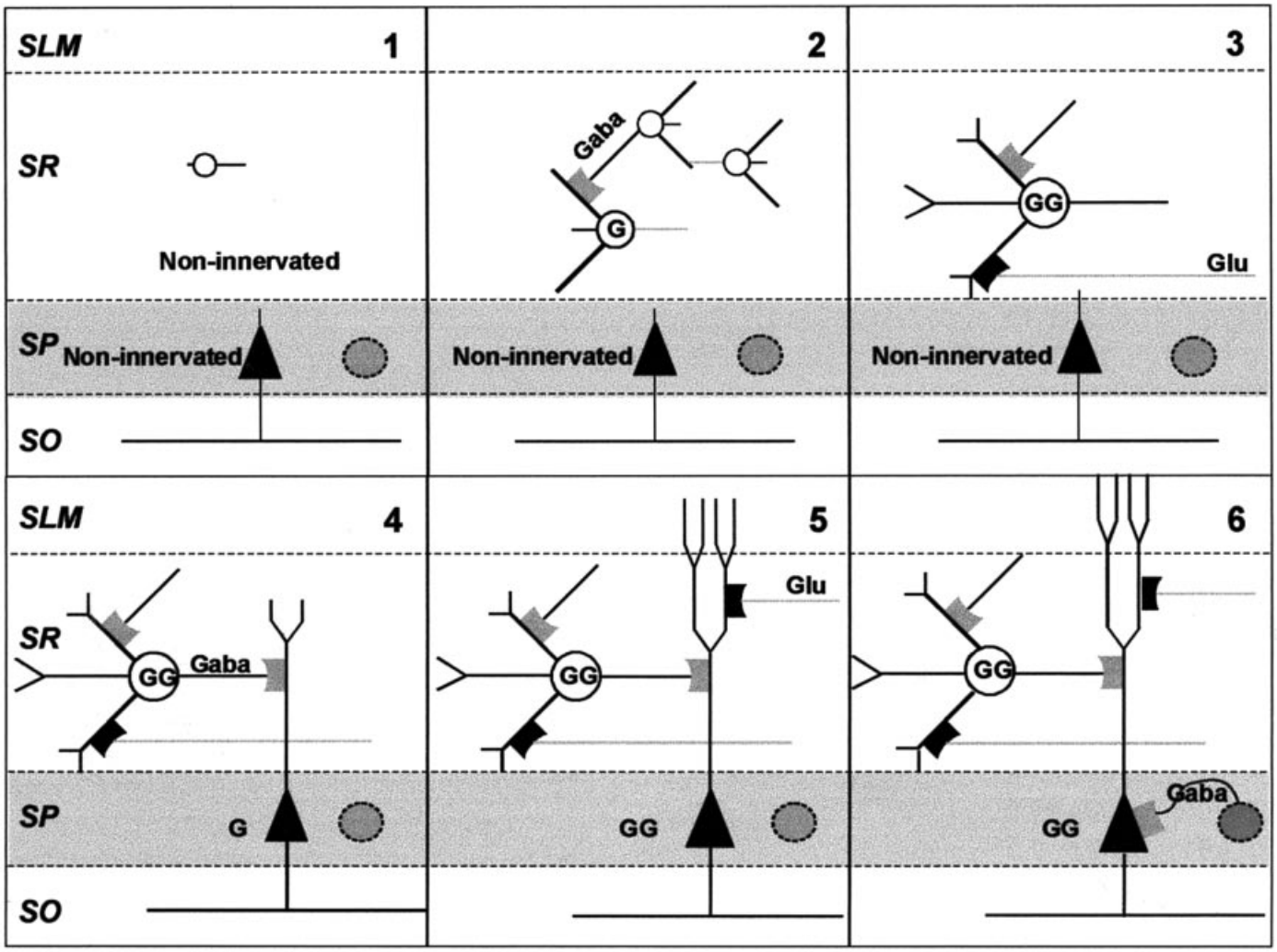

FIG. 9. Schematic representation of the sequential expression of $GABA_A$ and glutamatergic synapses in interneurons and pyramidal cells during development. This six-step diagram represents the events as they take place in one neuron of each type, but the heterogeneity within a given developmental stage is not taken into account. Interneurons are represented with a round cell body and pyramidal cells by a triangle. The doted circle in SP symbolizes a perisomatic interneuron. Step 1: both types are not yet innervated and have no functional synapses. Steps 2 and 3: the interneuron, but not the pyramidal cell, expresses sequentially $GABA_A$ (step 2) and glutamatergic (step 3) synapses; a network of functional interneurons is operative at this developmental stage. Steps 4 and 5: pyramidal neurons express sequentially $GABA_A$ (step 4) and glutamatergic (step 5) synapses on apical dendrites. Step 6: Perisomatic interneurons form $GABA_A$ synapses on the somata of the principal neurons.

the formation of glutamatergic synapses. Our results suggest that the degree of maturation of the target is essential for the maturation of glutamatergic synapses as suggested from cell cultures studies (Fletcher *et al*., 1994). These will be formed on the more mature interneurons prior to pyramidal neurons. The requirement for the maturation of unknown postsynaptic factors which selectively influence the formation of glutamatergic but not GABAergic synapses has been proposed recently (Mohrmann *et al*., 1999; Schinder *et al*., 2000). In addition, postsynaptic-associated proteins such as the PSD-95 protein-related family (see Ziv & Garner, 2001; Bresler *et al*., 2001), and other factors including neurotrophic factors or neuroligins that trigger synapse initiation may also be involved.

Peridendritic interneurons and synapses form prior to perisomatic ones

Morphofunctional results also suggest that peridendritic interneurons mature prior to perisomatic ones. Thus, a large majority of G-only or GG interneurons localized in SR have an axon that remains in the same region. Although the morphology of these neurons is highly heterogeneous, some of them may correspond to interneurons innervating other interneurons as their morphology resembles that of the different IS-type interneurons described previously (Freund & Buzsáki, 1996). Interneurons of this type are specialized to control other interneurons in the rat hippocampus and contain CR (Gulyás *et al*., 1996). In addition to presumably Cajal–Retzius cells, we found that CR is clearly expressed in P0 interneurons from SR, confirming previous results showing that this calcium-binding protein was present in embryonic and early postnatal stages (Jiang & Swann, 1997). Other interneurons may correspond to peridendritic interneurons which contribute to the early $GABA_A$ synapses that are located on the proximal part of apical pyramidal dendrites and not on the soma (Tyzio *et al*., 1999). The presence, in SR of CA1, of CB-immunoreactive cells that are known to innervate pyramidal cell dendrites (Freund & Buzsáki, 1996; Gulyas & Freund, 1996) and which have been reported consistently in other studies is in agreement with this suggestion. Also, none of the 162 reconstructed interneurons

extended a plexus of axonal ramification around the pyramidal cell layer, a hallmark of adult perisomatic cells (Freund & Buzsáki, 1996; Martinez *et al*., 1996). Furthermore, blind patch directly in the pyramidal layer did not reveal interneurons with a basket- or chandelier-like morphology. Synaptophysin (Tyzio *et al*., 1999) or GAD (Dupuy & Houser, 1996) immunoreactivities have not been detected in SP of P0 rats. Furthermore, in agreement with the observation that perisomatic interneurons are generated after other interneuron types (Soriano *et al*., 1986; Soriano *et al*., 1994), we found no PV-like immunoreactivity in P0 slices as previously reported (Nitsch *et al*., 1990; Solbach & Celio, 1991). Perisomatic interneurons may, however, be present at birth but, as reported, the expression of PV in these neurons coincides with the beginning of their physiological activity (Solbach & Celio, 1991), which occurs later (Nitsch *et al*., 1990). The conclusions derived from these observations is that the earlier formation of peridendritic interneurons correlates with the earlier formation of functional synapses on the dendrites of the principal cells (Tyzio *et al*., 1999) and that the different functions assigned to dendritic and somatic inhibitions (Miles *et al*., 1996) may also have a developmental gradient.

Long-range projections of interneurons

This study has also revealed interneurons with long axonal processes which project outside the CA1 region. They are also fully functional neurons with both $GABA_A$ and glutamate currents and via their wide dendritic and axonal arbors may provide direct interactions with distant cells located within the CA3 region, dentate gyrus or the subiculum. An immature form of interneuron identified in adult tissues (Freund & Buzsáki, 1996) can be recognized in some interneurons whereas others have no defined morphology and may either mature into other adult types or would disappear during postnatal development (Super *et al*., 1998). Thus, a neuron with O-LM-like morphology (61) has been recorded in P0 slices and the fact that SOM immunoreactivity has also been found in the SO of these slices is also in favour of the presence of this type of interneuron at birth. In addition, neurons resembling poorly developed back-projections (see Freund & Buzsáki, 1996) have been observed in P0 slices, and some interneurons were found to extend their axons in the subiculum region, suggesting that pyramidal cells are not the only neurons to contact this region at birth. Interestingly, the fissure does not appear to be a frontier between CA1 and DG as the axons and the dendrites of several interneurons were found to cross it and even to terminate in the granular cell layer. These neurons may contribute to maintaining intercommunications between brain areas. It is, however, not yet known whether they could also contribute to rhythm generation as reported in hippocampal cultures where the generation of GDPs was shown to require a small percentage of morphologically developed interneurons (Voigt *et al*., 2001).

Conclusion

Our study suggests that there is a developmental program of synapse formation which includes three developmental gradients: (i) the establishment of $GABA_A$ synapses prior to glutamatergic ones; (ii) their expression in interneurons before pyramidal neurons; and (iii) the establishment of peridendritic prior to perisomatic GABAergic synapses. The consequence of these multiple developmental steps is that, already at an early stage, interneurons are in a position to control the maturation of the hippocampal network, either via activity-dependent mechanisms and/or via signalling factors and messengers which may also be sequentially expressed. In the adult hippocampus, there is a wide range of behaviourally relevant patterns which are generated by interneurons and are determinant for the ongoing activity of the network (Buzsaki, 1997). We suggest that excitatory GABA already exerts a similar role in the forming hippocampal network when pyramidal cells are quiescent.

Acknowledgements

We thank I. Jorquera for neuronal reconstructions, S. Weller for providing the S-neuron software, A. Represa for immunocytochemistry experiments and R. Tyzio for his help in visual patch recordings.

Abbreviations

4-AP, 4-aminopyridine; ACSF, artificial cerebrospinal fluid; AMPA, α-amino-3-hydroxy-5-methyl-4-isoxazolepropionic acid; CA, cornu ammonis; CB, calbindin; CNQX, 6-cyano-7-nitro quinoxaline-2,3-dione; CR, calretinin; DAB, 3,3′-diaminobenzidine; D-APV, D-2-amino-5-phosphono pentanoic acid; E, embryonic day; GABA, gamma-aminobutyric acid; GDPs, giant depolarizing potentials; HEPES, N-2-hydroxyethyl-piperazine-N′-3-propane-sulphonic acid; NMDA, *N*-methyl-D-aspartate; O-LM, oriens lacunosum moleculare; P, postnatal day; PSC, postsynaptic current; PV, parvalbumin; SLM, stratum lacunosum moleculare; SO, stratum oriens; SOM, somatostatin; SP, stratum pyramidale; SR, stratum radiatum; TB, tris buffer; TBS, tris-buffered saline; TTX, tetrodotoxin.

References

Altman, J. & Bayer, S.A. (1990) Prolonged sojourn of developing pyramidal cells in the intermediate zone of the hippocampus and their settling in the stratum pyramidale. *J. Comp. Neurol.*, **301**, 343–364.

Barbin, G., Pollard, H., Gaiarsa, J.L. & Ben-Ari, Y. (1993) Involvement of $GABA_A$ receptors in the outgrowth of cultured hippocampal neurons. *Neurosci. Lett.*, **152**, 150–154.

Barker, J.L., Behar, T., Li, Y.X., Liu, Q.Y., Ma, W., Maric, D., Maric, I., Schaffner, A.E., Serafini, R., Smith, S.V., Somogyi, R., Vautrin, J.Y., Wen, X.L. & Xian, H. (1998) GABAergic cells and signals in CNS development. *Perspect. Dev. Neurobiol.*, **5**, 305–322.

Behar, T.N., Li, Y.X., Tran, H.T., Ma, W., Dunlap, V., Scott, C. & Barker, J.L. (1996) GABA stimulates chemotaxis and chemokinesis of embryonic cortical neurons via calcium-dependent mechanisms. *J. Neurosci.*, **16**, 1808–1818.

Belhage, B., Hansen, G.H., Elster, L. & Schousboe, A. (1998) Effects of gamma-aminobutyric acid (GABA) on synaptogenesis and synaptic function. *Perspect. Dev. Neurobiol.*, **5**, 235–246.

Ben-Ari, Y. (2001) Developing networks play a similar melody. *Trends Neurosci.*, **24**, 353–360.

Ben-Ari, Y., Cherubini, E., Corradetti, R. & Gaiarsa, J.L. (1989) Giant synaptic potentials in immature rat CA3 hippocampal neurones. *J. Physiol. (Lond.)*, **416**, 303–325.

Blasco-Ibanez, J.M. & Freund, T.F. (1995) Synaptic input of horizontal interneurons in stratum oriens of the hippocampal CA1 subfield: structural basis of feed-back activation. *Eur. J. Neurosci.*, **7**, 2170–2180.

Bresler, T., Ramati, Y., Zamorano, P.L., Zhai, R., Garner, C.C. & Ziv, N.E. (2001) The dynamics of sap90/psd-95 recruitment to new synaptic junctions. *Mol. Cell Neurosci.*, **18**, 149–167.

Buzsaki, G. (1997) Functions for interneuronal nets in the hippocampus. *Can. J. Physiol. Pharmacol.*, **75**, 508–515.

Chen, G., Trombley, P.Q. & Van den Pol, A.N. (1995) GABA receptors precede glutamate receptors in hypothalamic development; Differential regulation by astrocytes. *J. Neurophysiol.*, **74**, 1473–1484.

Davies, P., Anderton, B., Kirsch, J., Konnerth, A., Nitsch, R. & Sheetz, M. (1998) First one in, last one out: the role of gabaergic transmission in generation and degeneration. *Prog. Neurobiol.*, **55**, 651–658.

Diabira, D., Hennou, S., Chevassus-au-Louis, N., Ben-Ari, Y. & Gozlan, H. (1999) Late embryonic expression of AMPA receptor fonction in the CA1 region of the intact hippocampus in vitro. *Eur. J. Neurosci.*, **11**, 4015–4023.

Dupuy, S.T. & Houser, C.R. (1996) Prominent expression of two forms of glutamate decarboxylase in the embryonic and early postnatal rat hippocampal formation. *J. Neurosci.*, **16**, 6919–6932.

Fletcher, T.L., De Camilli, P. & Banker, G. (1994) Synaptogenesis in hippocampal cultures: evidence indicating that axons and dendrites become competent to form synapses at different stages of neuronal development. *J. Neurosci.*, **14**, 6695–6706.

Freund, T.F. & Buzsáki, G. (1996) Interneurons of the hippocampus. *Hippocampus*, **6**, 347–470.
Gulyas, A.I. & Freund, T.F. (1996) Pyramidal cell dendrites are the primary targets of calbindin D28k-immunoreactive interneurons in the hippocampus. *Hippocampus*, **6**, 525–534.
Gulyás, A.I., Hájos, N. & Freund, T.F. (1996) Interneurons containing calretinin are specialized to control other interneurons in the rat hippocampus. *J. Neurosci.*, **16**, 3397–3411.
Hamill, O.P., Marty, A., Neher, E., Sakmann, B. & Sigworth, F.J. (1981) Improved patch-clamp techniques for high-resolution current recording from cells and cell-free membrane patches. *Pflügers Arch.*, **391**, 85–100.
Jiang, M. & Swann, J.W. (1997) Expression of calretinin in diverse neuronal populations during development of rat hippocampus. *Neuroscience*, **81**, 1137–1154.
Katona, I., Acsady, L. & Freund, T.F. (1999) Postsynaptic targets of somatostatin-immunoreactive interneurons in the rat hippocampus. *Neuroscience*, **88**, 37–55.
Khazipov, R., Esclapez, M., Caillard, O., Bernard, C., Khalilov, I., Hirsch, J., Tyzio, R., Hirsch, J., Dzhala, V., Berger, B. & Ben-Ari, Y. (2001) Early development of neuronal activity in the primate hippocampus in utero. *J. Neurosci.*, **21**, 9770–9781.
Khazipov, R., Leinekugel, X., Khalilov, I., Gaiarsa, J.L. & Ben-Ari, Y. (1997) Synchronization of GABAergic interneuronal network in CA3 subfield of neonatal rat hippocampal slices. *J. Physiol. (Lond.)*, **498**, 763–772.
Koller, H., Siebler, M., Schmalenbach, C. & Muller, H.W. (1990) GABA and glutamate receptor development of cultured neurons from rat hippocampus, septal region, and neocortex. *Synapse*, **5**, 59–64.
Lang, U. & Frotscher, M. (1990) Postnatal development of nonpyramidal neurons in the rat hippocampus (areas CA1 and CA3): a combined Golgi/electron microscope study. *Anat. Embryol. (Berl.)*, **181**, 533–545.
Leinekugel, X., Medina, I., Khalilov, I., Ben-Ari, Y. & Khazipov, R. (1997) Ca^{2+} oscillations mediated by the synergistic excitatory actions of $GABA_A$ and NMDA receptors in the neonatal hippocampus. *Neuron*, **18**, 243–255.
Leinekugel, X., Tseeb, V., Ben-Ari, Y. & Bregestovski, P. (1995) Synaptic GABAA activation induces Ca^{2+} rise in pyramidal cells and interneurons from rat neonatal hippocampal slices. *J. Physiol. (Lond.)*, **487**, 319–329.
LoTurco, J.J., Owens, D.F., Heath, M.J.S., Davis, M.B.E. & Kriegstein, A.R. (1995) GABA and glutamate depolarize cortical progenitor cells and inhibit DNA synthesis. *Neuron*, **15**, 1287–1298.
Martinez, A., Del Lubke, J.R.J., Soriano, E. & Frotscher, M. (1996) Regional variability and postsynaptic targets of chandelier cells in the hippocampal formation of the rat. *J. Comp. Neurol.*, **376**, 28–44.
Miles, R., Toth, K., Gulyas, A.I., Hajos, N. & Freund, T.F. (1996) Differences between somatic and dendritic inhibition in the hippocampus. *Neuron*, **16**, 815–823.
Mohrmann, R., Werner, M., Hatt, H. & Gottmann, K. (1999) Target-specific factors regulate the formation of glutamatergic transmitter release sites in cultured neocortical neurons. *J. Neurosci.*, **19**, 10004–10013.
Nishimaru, H., Iizuka, M., Ozaki, S. & Kudo, N. (1996) Spontaneous motoneuronal activity mediated by glycine and GABA in the spinal cord of rat fetuses in vitro. *J. Physiol. (Lond.)*, **497**, 131–143.
Nitsch, R., Bergmann, I., Kuppers, K., Mueller, G. & Frotscher, M. (1990) Late appearance of parvalbumin-immunoreactivity in the development of GABAergic neurons in the rat hippocampus. *Neurosci. Lett.*, **118**, 147–150.
Owens, D.F., Liu, X. & Kriegstein, A.R. (1999) Changing properties of GABA (A) receptor-mediated signaling during early neocortical development. *J. Neurophysiol.*, **82**, 570–583.
Pena, F. & Tapia, R. (1999) Relationships among seizures, extracellular amino acid changes, and neurodegeneration induced by 4-aminopyridine in rat hippocampus: a microdialysis and electroencephalographic study. *J. Neurochem.*, **72**, 2006–2014.
Perreault, P. & Avoli, M. (1991) Physiology and pharmacology of epileptiform activity induced by 4-aminopyridine in rat hippocampal slices. *J. Neurophysiol.*, **65**, 771–785.
Schinder, A.F., Berninger, B. & Poo, M. (2000) Postsynaptic target specificity of neurotrophin-induced presynaptic potentiation. *Neuron*, **25**, 151–163.
Segal, M. (1993) GABA induces a unique rise of [Ca]i in cultured rat hippocampal neurons. *Hippocampus*, **3**, 229–238.
Solbach, S. & Celio, M.R. (1991) Ontogeny of the calcium binding protein parvalbumin in the rat nervous system. *Anat. Embryol. (Berl.)*, **184**, 103–124.
Soriano, E., Cobas, A. & Fairen, A. (1986) Asynchronism in the neurogenesis of GABAergic and non-GABAergic neurons in the mouse hippocampus. *Brain Res.*, **395**, 88–92.
Soriano, E., Del Rio, J.A., Martinez, A. & Super, H. (1994) Organization of the embryonic and early postnatal murine hippocampus. I. Immunocytochemical characterization of neuronal populations in the subplate and marginal zone. *J. Comp. Neurol.*, **342**, 571–595.
Storm, J.F. (1988) Temporal integration by a slowly inactivating K+ current in hippocampal neurons. *Nature*, **336**, 379–381.
Sudhof, T.C. (2001) alpha-Latrotoxin and its receptors: neurexins and CIRL/latrophilins. *Annu. Rev. Neurosci.*, **24**, 933–962.
Super, H., Martinez, A., Del Rio, J.A. & Soriano, E. (1998) Involvement of distinct pioneer neurons in the formation of layer-specific connections in the hippocampus. *J. Neurosci.*, **18**, 4616–4626.
Super, H. & Soriano, E. (1994) The organization of the embryonic and early postnatal murine hippocampus. II. Development of entorhinal, commissural, and septal connections studied with the lipophilic tracer DiI. *J. Comp. Neurol.*, **344**, 101–120.
Tyzio, R., Represa, A., Jorquera, I., Ben-Ari, Y., Gozlan, H. & Aniksztejn, L. (1999) The establishment of Gabaergic and glutamatergic synapses on CA1 pyramidal neurons is sequential and correlates with the development of the apical dendrite. *J. Neurosci.*, **19**, 10372–10382.
Voigt, T., Opitz, T. & de Lima, A.D. (2001) Synchronous oscillatory activity in immature cortical network is driven by GABAergic preplate neurons. *J. Neurosci.*, **21**, 8895–8905.
Walton, M.K., Schaffner, A.E. & Barker, J.L. (1993) Sodium channels, GABAA receptors, and glutamate receptors develop sequentially on embryonic rat spinal cord cells. *J. Neurosci.*, **13**, 2068–2084.
Ziv, N.E. & Garner, C.C. (2001) Principles of glutamatergic synapse formation: seeing the forest for the trees. *Curr. Opin. Neurobiol.*, **11**, 536–543.